DNA Sensors

DOI: 10.1002/anie.200604861

Microfluidic Control of Fluorescence Resonance Energy Transfer: Breaking the FRET Limit**

*Chun-yang Zhang and Lawrence W. Johnson**

Fluorescence resonance energy transfer (FRET) is unique in providing fluorescence signals sensitive to molecular conformation, association, and separation in the range of 1–10 nm.[1] FRET-based methods such as TaqMan and the molecular beacon assay have been widely used for the rapid detection of nucleic acids as they do not require separation of the unhybridized probes from target–probe hybrids;[2,3] however, both assays require two doubly labeled probes in close proximity which are hard to optimize and synthesize. The sandwich hybridization of donor-labeled oligonucleotide, acceptor-labeled oligonucleotide, and target oligonucleotides offers an alternative method for the homogenous assay of nucleic acids;[4] but the inherent dependence of FRET efficiency on Förster distance (R_0)[1] prevents the sensitive detection of long nucleic acids owing to the relatively small R_0 value for pairs of fluorescent dyes that are widely separated. The intervening "optical relay stations" or "midway fluorophores" in DNA oligonucleotides have been employed to accomplish multistep energy transfer over long distance,[5–8] but this method is complicated and not practicable for routine nucleic acid analysis.

Quantum dots (QDs) with unique optical properties such as size-tunable photoluminescence spectra and relatively high quantum yield[9] have shown promise as useful fluorophores in FRET-based sensing applications.[10–17] QD-based FRET assays have been developed for the detection of proteins and nucleic acids,[10–15] for monitoring the proteolytic activity[16] and for probing RNA–peptide interactions.[17] Electrical control of FRET between QDs and fluorescent dyes has been recently reported by Lupton et al. for the design of single-molecule optoelectronic switches.[18] The use of nanosensors to precisely control the FRET and further to break the FRET limit represents a significant challenge in nanotechnology. Here we report the microfluidic control of FRET and breaking of the FRET limit with a QD-based DNA nanosensor. We demonstrate that this nanosensor can sensitively detect long nucleic acids that are separated by a distance far beyond the useful range of FRET, without the involvement of a multistep mechanism.

[*] Dr. C. Y. Zhang, Prof. L. W. Johnson
Department of Chemistry, York College
and The Graduate Center
The City University of New York
Jamaica, NY 11451 (USA)
Fax: (+1) 718-262-2652
E-mail: lwj@york.cuny.edu

[**] This work was supported by NIH (GM08153).

Supporting information for this article is available on the WWW under http://www.angewandte.org or from the author.

In our nanosensor the streptavidin-coated 605-nm-emitting QD functions as both a nanoscaffold and a FRET donor (Figure 1a). The Alexa Fluor 647-labeled double-stranded DNAs (dsDNAs) were assembled on the 605QD surface by specific streptavidin–biotin binding. The binding of DNAs to

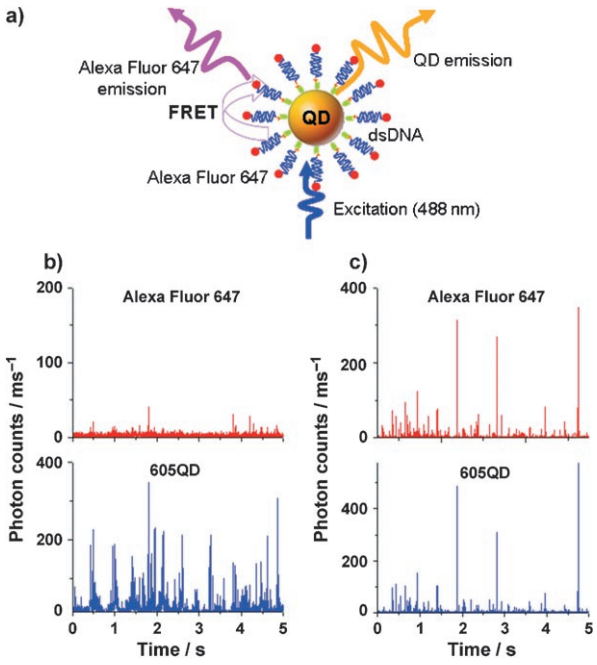

Figure 1. Principle of a QD-based DNA nanosensor. a) Conceptual scheme of single-QD-based DNA nanosensor. b) Representative traces of fluorescence bursts from 605QD/25-mer dsDNA/Alexa Fluor 647 complexes in a diffusion state. 605QD concentration: 1.0×10^{-10} M; concentration of Alexa Fluor 647-labeled 25-mer dsDNA: 1.8×10^{-9} M. c) Representative traces of fluorescence bursts from 605QD/25-mer dsDNA/Alexa Fluor 647 complexes in a microfluidic flow. Flow rate: 4.0 μL min^{-1}; 605QD concentration: 2.0×10^{-11} M; concentration of Alexa Fluor 647-labeled 25-mer dsDNA: 3.6×10^{-10} M.

605QD resulted in the formation of 605QD/dsDNA/Alexa Fluor 647 complexes. Upon excitation with a wavelength of 488 nm, FRET occurred between the 605QD and the Alexa Fluor 647; the fluorescence signals of 605QD and Alexa Fluor 647 were observed simultaneously. The selection of the 605QD/Alexa Fluor 647 FRET pair produced negligible cross-talk between the donor and acceptor emissions, and the broad absorption band of 605QD allowed sample excitation at 488 nm without direct excitation of Alexa Fluor 647 (see Figure S1 in the Supporting Information).

Single-molecule detection of 605QD/25-mer dsDNA/Alexa Fluor 647 complexes in a diffusion state (Figure 1b)

was compared to that in a microfluidic flow (Figure 1c) at the DNA/605QD ratio of 18:1. A few low fluorescence bursts from Alexa Fluor 647 were observed from diffusing 605QD/25-mer dsDNA/Alexa Fluor 647 complexes (Figure 1b); the mean FRET efficiency (E) was only $(9.10 \pm 0.45)\%$. In contrast, more and higher fluorescence bursts from Alexa Fluor 647 were observed in a microfluidic flow, and each Alexa Fluor 647 burst had a corresponding 605QD burst (Figure 1c). The mean E value of $(42.98 \pm 0.21)\%$ in a microfluidic flow was much higher than that from a diffusion state, suggesting the significant effect of microfluidic flow upon FRET.

To investigate the microfluidic control of FRET, we studied the effect of flow rate on the FRET efficiency of 605QD/25-mer dsDNA/Alexa Fluor 647 complexes. The autocorrelation curve of 605QD was measured by fluorescence correlation spectroscopy (FCS) at different pump speeds. The flow velocity was obtained by fitting the autocorrelation curves of 605QD to the FCS-flow model (Figure 2a).[19,20] A linear correlation was obtained between the pump speed and the calculated flow velocity (Figure 2b), suggesting the

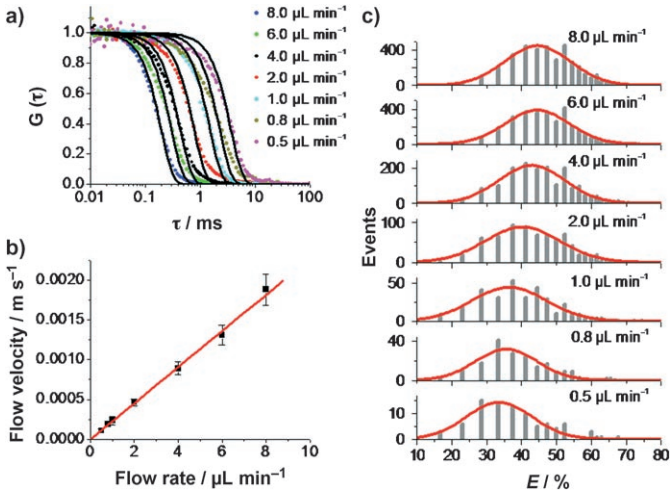

Figure 2. Microfluidic control of FRET. a) Normalized autocorrelation functions calculated from fluorescence intensity trajectories of 605QD (dotted lines) along with the fits to the flow model (solid lines) at different flow rates. b) Linearity of flow velocities obtained from analysis with FCS-flow model versus the applied flow rate through the capillary. c) Histograms of measured FRET efficiency for 605QD/25-mer dsDNA/Alexa Fluor 647 complexes as a function of increasing flow rate. The red curves represent the fit of experimental data to Gaussian function. 605QD concentration: 5.0×10^{-11} M; concentration of Alexa Fluor 647-labeled 25-mer dsDNA: 9.0×10^{-10} M.

accurate tuning of flow velocity by the pump speed (the flow rate was simply described as the pump speed in this paper). We generated the histograms of FRET efficiencies (E) at different flow rates and extracted the mean value of each histogram by fitting it to a Gaussian distribution. As shown in Figure 2c, the mean E value shifted from $(33.37 \pm 0.24)\%$ at a flow rate of 0.5 μL min^{-1} to $(44.54 \pm 0.18)\%$ at a flow rate of 6.0 μL min^{-1}, indicating that the FRET efficiency improved with increasing flow rate. The calculation of donor–acceptor separation distance (r) from the mean E revealed that r decreased from (129.89 ± 0.31) Å at a flow rate of 0.5 μL min^{-1} to (120.05 ± 0.22) Å at a flow rate of 6.0 μL min^{-1}, suggesting that the enhanced FRET efficiency was attributed to a flow-induced reduction in donor–acceptor separation distance, which was caused by the deformation of DNA molecules in the Poiseuille flow.[21] Further increase of flow rate from 6.0 μL min^{-1} to 8.0 μL min^{-1} did not lead to significant improvement in FRET efficiency (mean E of $44.60 \pm 0.16\%$ at flow rate of 8.0 μL min^{-1}), indicating that the overall distance between Alexa Fluor 647 and 605QD had reached its minimum limit. Further experiments revealed that the mean E shifted to a lower value when the focus position of laser beam moved from the center of the capillary to the edge of the wall (see Figure S2 in the Supporting Information). This decrease in mean E was consistent with the parabolic velocity profile of capillary flow, which had its highest flow velocity in the center of capillary and a lower velocity near the wall.[20] These experiments clearly demonstrate that the FRET between 605QD and Alexa Fluor 647 can be simply controlled by varying the flow rate, thus paving the way to improving the detection sensitivity of the QD-based FRET assays.

We further employed this QD-based nanosensor to detect long DNA which had separation distances far beyond the range of FRET. As a proof of concept, one 50-base target oligonucleotide was sandwich-hybridized to one 25-base biotinylated capture probe and one 25-base Alexa Fluor 647-labeled reporter probe to form a 50-mer dsDNA with contour length of 17.0 nm. After addition of the streptavidin-coated 605QD with a radius of 5.0–7.5 nm,[22] the separation distance between 605QD donor and Alexa Fluor 647 acceptor was 22.0–24.5 nm, even without taking into account the contribution of the biotin (Figure 3a). This separation distance is far beyond the useful range of FRET ($2R_0 = 14.3$ nm);[23] in principle FRET cannot occur between 605QD and Alexa Fluor 647 in this 605QD/50-mer dsDNA/Alexa Fluor 647 complex. Indeed, this was true for ensemble measurements. Figure 3b shows that the 605QD fluorescence did not decrease despite the increase of the ratio of Alexa Fluor 647-labeled dsDNA to 605QD. This indicates that no FRET occurred between 605QD and Alexa Fluor 647 in the 605QD/50-mer dsDNA/Alexa Fluor 647 complexes (For comparison, the 605QD/25-mer dsDNA/Alexa Fluor 647 complexes with shorter separation distance displayed distinct FRET between 605QD and Alexa Fluor 647 in the ensemble measurements; see Figure S3 in the Supporting Information). Surprisingly, in measurements with single-molecule detection in a microfluidic flow, distinct Alexa Fluor 647 bursts were observed in the 605QD/50-mer dsDNA/Alexa Fluor 647 complexes, and each one had a corresponding 605QD burst (Figure 4a). Consequently FRET did occur between Alexa Fluor 647 and 605QD in the 605QD/50-mer dsDNA/Alexa Fluor 647 complexes. The average donor–acceptor separation distance in microfluidic flow was calculated to be (12.60 ± 0.70) nm, much shorter than that in the ensemble measurement (22.0–24.5 nm). The breaking of the FRET limit in the microfluidic flow was thus attributed to the flow-induced deformation of DNA,[21] which put Alexa Fluor 647 spatially

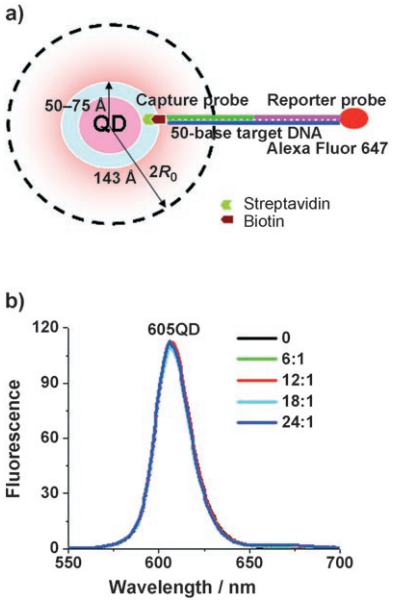

Figure 3. FRET limit prevents the detection of 50-mer dsDNA in ensemble measurements. a) A scheme depicting the separation distance in the 605QD/50-mer dsDNA/Alexa Fluor 647 complexes in which the 50-base target oligonucleotide is assembled on the surface of 605QD by DNA sandwich hybridization. b) Evolution of the fluorescence spectra from 605QD and Alexa Fluor 647 as a function of the increasing DNA/605QD ratio in 605QD/50-mer dsDNA/Alexa Fluor 647 complexes. 605QD concentration: 3.3×10^{-8} M; concentration of Alexa Fluor 647-labeled 50-mer dsDNA was varied with the DNA/605QD ratio as shown.

closer to 605QD. In the control experiments without the targets, there were only the 605QD bursts from the donor channel; there were no Alexa Fluor 647 bursts from the acceptor channel since there was no dye sandwiched to the 605QD (Figure 4b). Figure 4c showed the histogram of FRET efficiency as a function of the increasing DNA/605QD ratio; the mean E value shifted from (16.06 ± 0.24)% at a DNA/605QD ratio of 1:1 to (36.76 ± 0.10)% at a ratio of 24:1. This was due to the improved FRET efficiency as a consequence of the increase in the number of dye molecules per QD.[12] As shown in Figure 4d, the Alexa Fluor 647 burst counts increased as a function of the increasing DNA/605QD ratio as well, suggesting high sensitivity of this QD-based nanosensor for detection of extended strands of DNA. These experiments clearly demonstrate that this QD-based nanosensor can not only break the FRET limit, but also distinguish even one copy differences of long target oligonucleotides that are sandwiched to 605QD.

So far great efforts have been put into precisely controlling FRET and circumventing the FRET limit.[5–8,24] In addition to the optical approaches of intervening "midway fluorophores",[5–8] a micromechanical method has also been developed,[24] but it can only detect single-hybridization events independent of target concentration, making it unsuitable for routine quantitative analysis. In contrast, our method has the advantage of being technically simpler and suitable for high-throughput quantitative analysis. This assay can be easily expanded to microfluidic chips to form a platform for a sensitive DNA-array-based assay. Microfluidic control of FRET and breaking the FRET limit open up a new avenue for rapid, sensitive, and homogenous analysis of long nucleic acids whose detection is not feasible with conventional FRET-based assays (for example, QD-based ensemble measurements and fluorescent dye-based FRET assays). This approach should find wide application in the sensitive detection of unamplified genomic nucleic acids from bacteria, viruses, and cancer cells in clinical diagnostics and medical research.

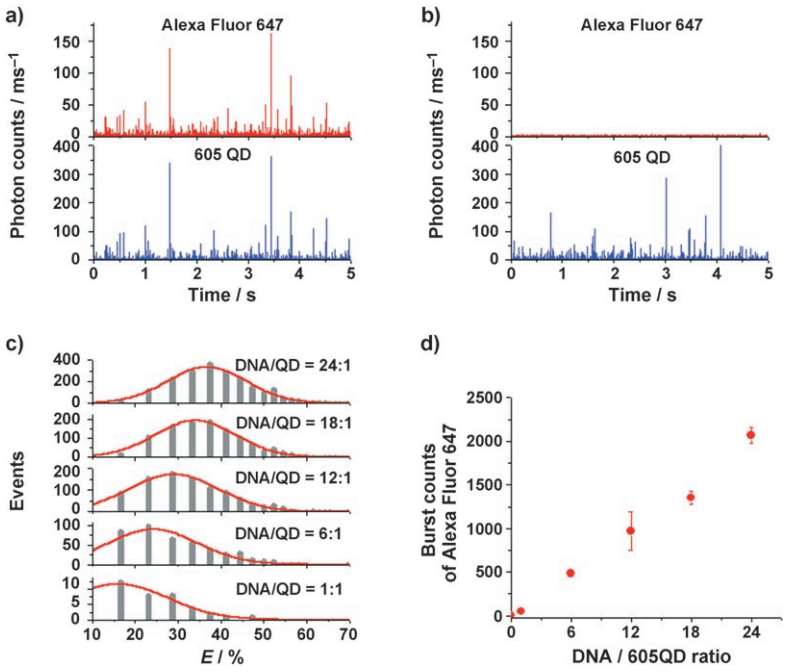

Figure 4. Breaking the FRET limit in a microfluidic flow. a) Representative traces of fluorescence bursts from 605QD/50-mer dsDNA/Alexa Fluor 647 complexes in a microfluidic flow. Flow rate: 4.0 μL min^{-1}; 605QD concentration: 5.0×10^{-11} M; concentration of Alexa Fluor 647-labeled 50-mer dsDNA: 9.0×10^{-10} M. b) Representative traces of fluorescence bursts from the control group in the absence of target DNA. c) Histograms of measured FRET efficiency for 605QD/50-mer dsDNA/Alexa Fluor 647 complexes as a function of DNA/605QD ratio. 605QD concentration: 5.0×10^{-11} M; concentration of Alexa Fluor 647-labeled 50-mer dsDNA was varied with the DNA/605QD ratio as shown. d) The variance of Alexa Fluor 647 burst counts with the DNA/605QD ratio. Error bars show the standard deviation of three experiments.

Received: November 30, 2006
Published online: March 27, 2007

Keywords: biosensors · DNA recognition · FRET (fluorescence resonant energy transfer) · nanotechnology

[1] L. Stryer, *Annu. Rev. Biochem.* **1978**, *47*, 819–846.
[2] P. M. Holland, R. D. Abramson, R. Watson, D. H. Gelfand, *Proc. Natl. Acad. Sci. USA* **1991**, *88*, 7276–7280.
[3] S. Tyagi, F. R. Kramer, *Nat. Biotechnol.* **1996**, *14*, 303–308.
[4] R. A. Cardullo, S. Agrawal, C. Flores, P. C. Zamecnik, D. E. Wolf, *Proc. Natl. Acad. Sci. USA* **1988**, *85*, 8790–8794.

[5] S. Kawahara, T. Uchimaru, S. Murata, *Chem. Commun.* **1999**, 6, 563 – 564.
[6] A. K. Tong, Z. Li, G. S. Jones, J. J. Russo, J. Ju, *Nat. Biotechnol.* **2001**, *19*, 756 – 759.
[7] A. K. Tong, S. Jockusch, Z. Li, H. R. Zhu, D. L. Akins, N. J. Turro, J. Ju, *J. Am. Chem. Soc.* **2001**, *123*, 12923 – 12924.
[8] M. Heilemann, P. Tinnefeld, G. S. Mosteiro, M. G. Parajo, N. F. V. Hulst, M. Sauer, *J. Am. Chem. Soc.* **2004**, *126*, 6514 – 6515.
[9] I. L. Medintz, H. T. Uyeda, E. Goldman, H. Mattoussi, *Nat. Mater.* **2005**, *4*, 435 – 446.
[10] I. L. Medintz, A. R. Clapp, H. Mattoussi, E. R. Goldman, B. R. Fisher, J. M. Mauro, *Nat. Mater.* **2003**, *2*, 630 – 638.
[11] I. L. Medintz, J. H. Konnert, A. R. Clapp, I. Stanish, M. E. Twigg, H. Mattoussi, J. M. Mauro, J. R. Deschamps, *Proc. Natl. Acad. Sci. USA* **2004**, *101*, 9612 – 9617.
[12] A. R. Clapp, I. L. Medintz, J. M. Mauro, B. R. Fisher, M. G. Bawewndi, H. Mattoussi, *J. Am. Chem. Soc.* **2004**, *126*, 301 – 310.
[13] C. Y. Zhang, H. C. Yeh, M. T. Kuroki, T. H. Wang, *Nat. Mater.* **2005**, *4*, 826 – 831.
[14] R. Bakalova, Z. Zhelev, H. Ohba, Y. Baba, *J. Am. Chem. Soc.* **2005**, *127*, 11328 – 11335.
[15] S. Hohng, T. Ha, *ChemPhysChem* **2005**, *6*, 956 – 960.
[16] I. L. Medintz, A. R. Clapp, F. M. Brunel, T. Tiefenbrunn, H. T. Uyeda, E. L. Chang, J. R. Deschamps, P. E. Dawson, H. Mattoussi, *Nat. Mater.* **2006**, *5*, 581 – 589.
[17] C. Y. Zhang, L. W. Johnson, *J. Am. Chem. Soc.* **2006**, *128*, 5324 – 5325.
[18] K. Becker, J. M. Lupton, J. Müller, A. L. Rogach, D. V. Talapin, H. Weller, J. Feldmann, *Nat. Mater.* **2006**, *5*, 777 – 781.
[19] P. C. Brister, K. K. Kuricheti, V. Buschman, K. D. Weston, *Lab Chip* **2005**, 5, 785 – 791.
[20] B. H. Kunst, A. Schots, A. J. W. G. Visser, *Anal. Chem.* **2002**, *74*, 5350 – 5357.
[21] J. J. Zheng, E. S. Yeung, *Anal. Chem.* **2002**, *74*, 4536 – 4547.
[22] Qdot streptavidin conjugates user manual, PN 90-0003 Rev 5, Quantum Dot Corp. Hayward, CA.
[23] T. T. Nikiforov, J. M. Beechem, *Anal. Biochem.* **2006**, *357*, 68 – 76.
[24] M. Singh-Zocchi, S. Dixit, V. Ivanov, G. Zocchi, *Proc. Natl. Acad. Sci. USA* **2003**, *100*, 7605 – 7610.

